

WINDS, BUBBLES, ... BUT MAGNETIZED: SOLUTIONS FOR HIGH SPEED POST-AGB WINDS AND THEIR EXTREME COLLIMATION

G. García-Segura,¹ J. A. López,¹ and J. Franco²

RESUMEN

Este artículo propone soluciones para el origen de los vientos de estrellas del tipo post-AGB, su aceleración hasta alta velocidad, y la subsecuente formación de nebulosas protoplanetarias altamente colimadas. Se calculan varios modelos de vientos con velocidades terminales desde algunas decenas de km s^{-1} hasta de 10^3 km s^{-1} , los cuales producen nebulosas protoplanetarias con momentos lineales en el rango 10^{36} a $10^{40} \text{ g cm s}^{-1}$ y energías cinéticas en el rango 10^{42} a 10^{47} erg . Estos resultados concuerdan con las observaciones disponibles de nebulosas protoplanetarias. En el esquema simple que se plantea, la presión magnética en la superficie estelar es la única causa de los vientos. En este estudio no se tienen en cuenta otros tipos de fuerzas, excepto la gravedad. La conclusión del estudio es que, tanto las tasas de pérdida de masa de las estrellas del tipo post-AGBs como los tiempos de transición entre las fases tardías de estrellas tipo AGB y estrellas centrales de nebulosas planetarias pueden estar directamente ligadas a la producción de campo magnético en los núcleos estelares. Como ejemplo, se predicen tasas de pérdida de masa tan altas como $8 \times 10^{-5} M_{\odot} \text{ yr}^{-1}$, y tiempos de transición tan cortos como 5000 años.

ABSTRACT

This paper provides solutions for the origin of post-AGB winds, their acceleration up to high speed, and the subsequent formation of extremely collimated proto-planetary nebulae. Several wind models with terminal velocities from a few tens of km s^{-1} up to 10^3 km s^{-1} are calculated, which produce proto-planetary nebulae with linear momenta in the range 10^{36} to $10^{40} \text{ g cm s}^{-1}$ and with kinetic energies in the range 10^{42} to 10^{47} erg . These results match available observations of proto-planetary nebulae. In the present simplistic scheme, the driver of the wind is just the magnetic pressure at the stellar surface. Other forces are not taken into account in this study, except gravity. We conclude that mass-loss rates of post-AGB stars and transition times from late AGB up to planetary nebula central stars could be directly linked with the production of magnetic field at the stellar core. As an example, mass-loss rates as large as $8 \times 10^{-5} M_{\odot} \text{ yr}^{-1}$ and transition times as short as 5000 years are predicted.

Key Words: ISM: BUBBLES — ISM: JETS AND OUTFLOWS — STARS: AGB, POST-AGB — STARS: MASS LOSS

1. INTRODUCTION

Classically, it has been accepted in the literature that planetary nebulae (PNs) are powered by line-driven winds emerging from their central stars, in the form of a two-wind dynamic interaction (Kwok, Purton, & Fitzgerald 1978). Evidences for this scenario are the large number of P Cygni line profiles detected in the central objects (see review by Perinotto 1983).

On the other hand, winds from asymptotic giant branch (AGB) stars are thought to be driven by radiation pressure on dust grains (see review by Habing 1996), although an alternative physical mechanism has been proposed by Pascoli (1997) based on the magnetic pressure at the stellar surface, which is transported out from the stellar interior.

Proto-planetary nebulae (PPNs) are transitional objects, and one could think that they are also powered by radiation pressure. However, observations of PPNs (Alcolea et al. 2001; Bujarrabal et al. 2001 and references therein) reveal that the linear momenta and kinetic energies associated with those nebulae are extremely large. Specifically, from a total sample of 32 PPNs studied in Bujarrabal et al. (2001), 80% of those PPNs have momenta that are too large to be powered by radiation pressure, in several cases up to three orders of magnitude. They do not match with radiation pressure on dust grains, line-driven winds or continuum-driven winds. This basic problem has been discussed in detail by Bujarrabal et al. (2001), and there is still no clear candidate for a possible driver.

Pascoli's (1997) results offer an alternative for the large amount of mass lost by AGB stars, and

¹Instituto de Astronomía, UNAM, Ensenada, México.

²Instituto de Astronomía, UNAM, México D.F., México.

it is logical to make an extension to the case of post-AGB stars, provided that the generation of magnetic fields could be even more efficient in post-AGB stars (Blackman et al. 2001). OH maser radio observations of the PPN K 3-35 (Miranda et al. 2001) reveal the existence of circular polarization attributed to the Zeeman effect, proving the existence of magnetic field in PPNs, while radio observations of CRL 2688 and NGC 7027 by Greaves (2002) proved that the magnetic fields in both objects are predominantly toroidal, in accordance with Pascoli's results. Thus, magnetic-driven winds could be a reasonable solution for the origin of PPNs.

In previous papers (Różyczka & Franco 1996; García-Segura 1997; García-Segura et al. 1999; García-Segura & López 2000; García-Segura, López, & Franco 2001), we assumed magnetized line-driven winds in the range 10^2 to 10^3 km s $^{-1}$ in which the magnetic field was entirely radial at the stellar surface, and it did not play an important role near the star, only at large distances. Those solutions were used to model planetary nebulae with hot central stars, where line-driven winds should operate. Blackman et al. (2001) also proposed that the fields should be primarily poloidal and parallel to the flow at small distances from the star, whereas at large distances one would expect a dominant toroidal component. In Blackman et al. (2001), the post-AGB wind is produced by magneto-centrifugal processes when the AGB star sheds its outer layers and exposes the rapidly rotating, magnetized core.

In the present work, we consider a different approach to the problem in accordance with Pascoli (1997). The wind is computed from the stellar surface, and it is solved from sonic velocity up to the terminal velocity. For simplicity, the toroidal magnetic field at the stellar surface is the main and only driver of the wind. This is probably an ideal, simplified case, but it allows us to quantify the pure effect of the magnetic field. The effects of radiation pressure acting together with the magnetic field, and the contribution of a poloidal component of the field will be the subject of a future paper.

2. NUMERICAL MODELS

The novel aspect in this paper with respect to our previous ones (Różyczka & Franco 1996; García-Segura 1997; García-Segura et al. 1999; García-Segura & López 2000; García-Segura et al. 2001) is that a stellar wind is not imposed at the inner boundary, rather, the wind is computed in a simple manner.

In order to do so, we initially set a cold (100 K), isothermal atmosphere, which obeys a power law in the form $\rho \sim r^{-2}$, with outward sonic velocity i.e., the initial conditions are almost stationary. The stellar gravitational field is included as an external force, which corresponds to that of a point mass of $1 M_{\odot}$. Note that under these conditions, the whole atmosphere will collapse in a free-fall timescale if no other forces are included. Once the grid is filled with the above conditions, a toroidal magnetic field is introduced at the stellar surface

$$B_{\phi}(\theta) = B_s \sin \theta, \quad (1)$$

where B_s is the field at the equator. Note that the surface magnetic field B_s introduced in previous papers corresponded to the radial component of the field, while in this paper it is an already purely toroidal component, following Pascoli (1997). It is precisely the magnetic pressure ($\sim B_s^2$) introduced at the stellar surface which causes the atmosphere to expand, and the result of this is a pure, magnetically-driven stellar wind. Note that radiation pressure has not been taken into account in this study, whose only purpose is to isolate pure magnetic effects. A more realistic model will include the effects of both, but this is beyond the scope of the present paper.

To compute the time evolution of above initial conditions, we have performed the simulations using the magnetohydrodynamic code ZEUS-3D (version 3.4), developed by M. L. Norman and the Laboratory for Computational Astrophysics. This is a finite-difference, fully explicit, Eulerian code descended from the code described in Stone & Norman (1992). A method of characteristics is used to compute magnetic fields, as described in Clarke (1996), and flux freezing is assumed in all the runs. We have used spherical polar coordinates (r, θ, Φ) , with reflecting boundary conditions at the equator and the polar axis. Rotational symmetry is assumed with respect to the polar axis, and our models are effectively two-dimensional. The simulations are carried out in the meridional (r, θ) plane, but three independent components of the velocity and magnetic field are computed (i.e., the simulations are "two and a half" dimensions).

3. RESULTS

3.1. Post-AGB Wind Models

We have first verified our method using as input stellar conditions the ones used by Pascoli (1997) for an AGB star, which are: $M = 1.1 M_{\odot}$, $R_s = 2$ AU, $B_s = 40$ G, and $\rho_s = 3.5 \times 10^{-10}$ g cm $^{-3}$.

TABLE 1
MODEL PARAMETERS

Model	B_s G	v_∞ ($40 R_s$) km s^{-1}	\dot{M} $M_\odot \text{yr}^{-1}$	M_s M_\odot	R_s AU
A	0.1	34	1.6×10^{-6}	1.0	4.5
B	1.0	374	1.67×10^{-5}	1.0	4.5
C	5.0	1874	8.35×10^{-5}	1.0	4.5

Our grid consists of 200×180 equidistant zones in r and θ , respectively. The innermost radial zone lies at $r_i = 2 \text{ AU}$, just at the stellar surface, and the outermost zone at $r_o = 80 \text{ AU}$. The angular extent is 90° in each case.

For those values, we obtain a similar result for the asymptotic velocity $v_\infty = 17.7 \text{ km s}^{-1}$ at $r = 40 R_s$ (i.e., 80 AU), inside the range 10 to 20 km s^{-1} obtained by Pascoli (1997). Our solution agrees in shape with his Figure 3 (case $1/x^2$).

The next step is to select a prototype stellar candidate to compute solutions for post-AGB winds. We have selected from the literature the very well studied object OH 231.8+4.2 (Sánchez-Contreras, Bujarrabal, & Alcolea 1997; Alcolea et al. 2001; Bujarrabal et al. 2002; Jura, Chen, & Plavchan 2002; Desmurs et al. 2002), which has a cool (M9III, $T \sim 2000 \text{ K}$) central star with $M \approx 1 M_\odot$, $R_s = 4.5 \text{ AU}$, and a rotation velocity of $v_{\text{rot}} = 6 \text{ km s}^{-1}$, member of the open cluster NGC 2437 (M 46), with an estimated initial mass of $M_{\text{ZAMS}} = 3 M_\odot$.

We have computed three wind solutions (A, B, C), in which the imposed stellar magnetic fields are 0.1, 1, and 5 G, respectively (Table 1).

The asymptotic terminal velocity has been measured at $r = 40 R_s$ just above the equatorial plane. To compute the mass-loss rate, we have solved the integral

$$\dot{M}(r) \equiv \int_0^{\pi/2} \dot{m}(r, \theta) \sin \theta d\theta \quad (2)$$

at $r = 40 R_s$, where

$$\dot{m}(r, \theta) \equiv 4\pi\rho(r, \theta) v_\infty(r, \theta) r^2. \quad (3)$$

These solutions are computed with a fixed grid, in which the innermost radial zone lies at $r_i = 4.5 \text{ AU}$, just at the stellar surface, and the outermost zone at $r_o = 180 \text{ AU}$ (i.e., $40 R_s$), up to the point where the solutions become stationary in time.

These calculations show the feasibility for toroidal magnetic fields to originate winds from a few tens of km s^{-1} up to 10^3 km s^{-1} for cool stars,

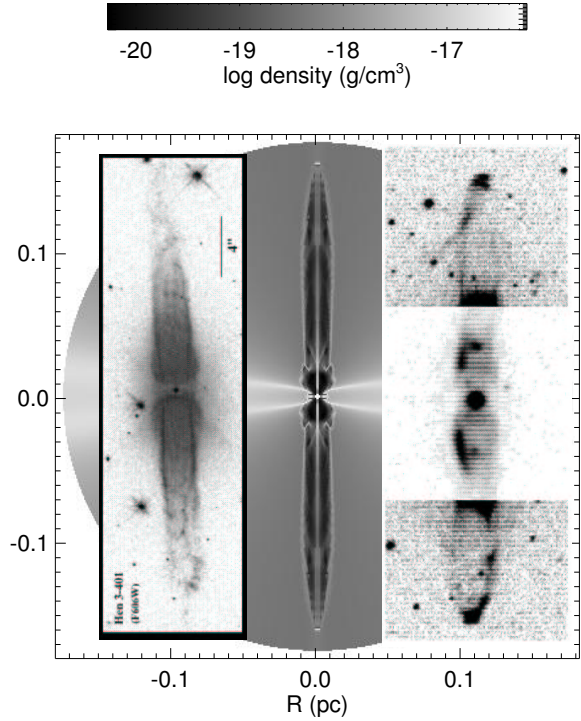


Fig. 1. Logarithm of density for model B (1 G) after 1000 yr of evolution (center) in comparison with observations of He 3-401 (Sahai 2002: left) and M 2-9 (Schwarz et al. 1997: right).

in which line-driven winds are not effective and radiation pressure on dust grains does not provide fast solutions.

3.2. Proto-Planetary Nebula Models

The next step is to calculate the type of nebulae that previous post-AGB wind models are able to originate.

A self-expanding grid technique has been used in order to allow a large range in the spatial coordinate of several orders of magnitude. Our expanding grids consist of 200×180 equidistant zones in r and θ , respectively. The innermost radial zone lies at $r_i = 4.5 \text{ AU}$, just at the stellar surface, and the outermost zone lies initially at $r_o = 180 \text{ AU}$. These values are used only up to the point where a shock approaches the outer boundary. After that, a shock tracking routine evaluates the expansion velocity of each forward shock (v_s) at the polar axis and produces a self-expanding grid using $vg(i) = v_s(r(i)/r_s)$, where $vg(i)$ and $r(i)$ are the velocity and position of each grid zone in the r -coordinate, and r_s is the position of the shock wave. Thus, the final grid size

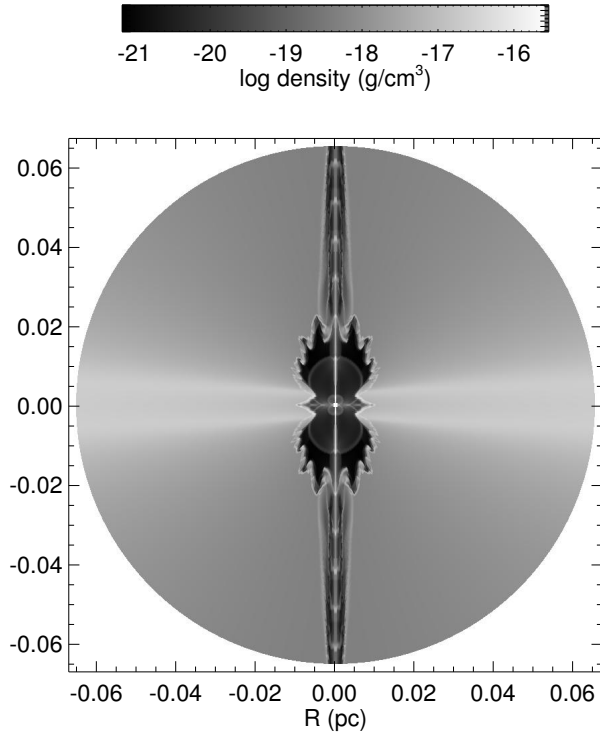


Fig. 2. Logarithm of density for model B (1 G) at 1000 yr, but with a magnetic cycle of 80 years. Every 40 years a blob is formed at the polar axis.

depends on the dynamical evolution for each individual run. The angular extent is 90° in each case.

As an example, in Figure 1 we show the solution of a numerical simulation for model B at 1000 yr from the onset of the fast wind, in which the imposed field is 1 G at the stellar surface. The solution is an extremely collimated nebula, similar in shape, size and kinematics to He 3-401 and M 2-9 (see the figure for direct comparison).

4. MAGNETIC CYCLES

We have computed (Figure 2) a model with a simple treatment of the stellar magnetic field B_s , which is allowed to change sign in a cycle of the form:

$$B_s(t) = B_{\max} \cos(2\pi \frac{t}{P}), \quad (4)$$

where B_{\max} is the maximum average B -field at the stellar surface, and P is the period of the magnetic cycle. Since we do not know the true variational form of the field, this functional form is just a simple first approximation. As in the case of the Sun, we assume that B_{\max} has opposite signs in each hemisphere, with a neutral current sheet near the equatorial plane (e.g., Wilcox & Ness 1965; Smith, Tsurutani, & Rosenberg 1978). Its average thickness in

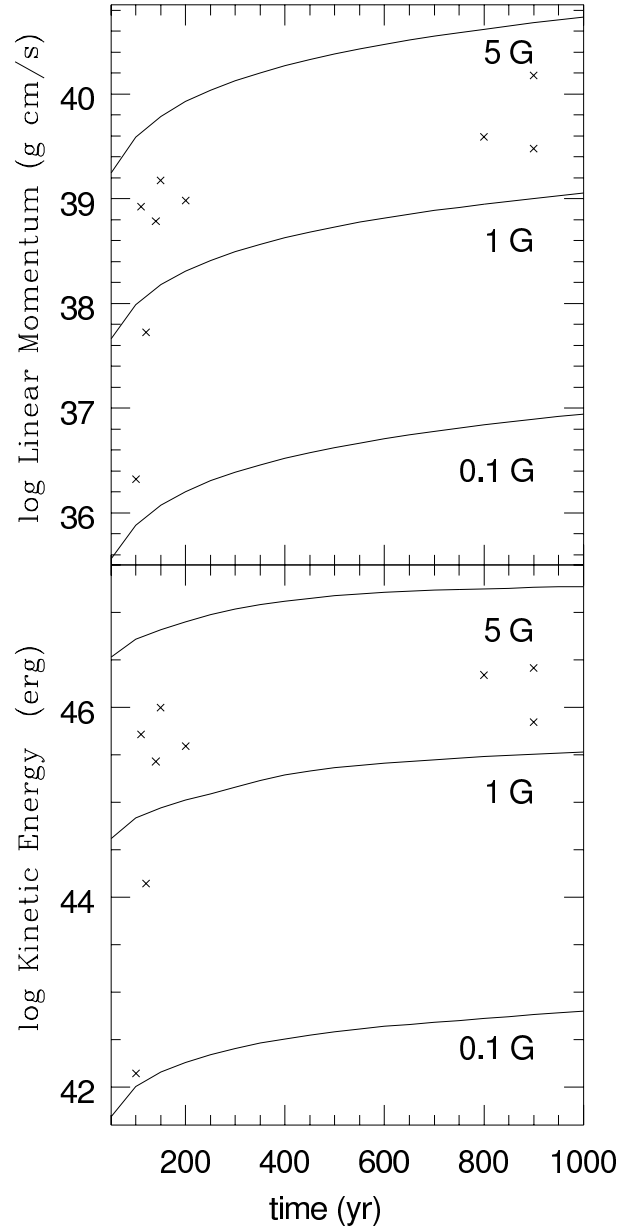


Fig. 3. Evolution of total linear momentum (top) and total kinetic energy (bottom) gained by models A (0.1 G), B (1 G) and C (5 G). Available observations (crosses) are taken from Bujarrabal et al. (2001).

the Solar case is of about 10^8 cm, and its presence does not affect the field outside the equatorial sections. For simplicity, given that we compute only one hemisphere, we neglect the size of this current sheet.

We have used a period of 80 yr. This value is actually taken from Sahai et al. (2002) to match the case of He 2-90. Fig. 2 shows the formation of a highly collimated nebula, which shows a knotty jet

inside the bubble. The knot separations are 40 yr in time, which corresponds to one half of the period imposed for the magnetic cycle.

5. DISCUSSION

It is important to compute the kinetic energy and linear momentum resulting from the models in order to compare with the available observations of PPNs (Bujarrabal et al. 2001). Both quantities are plotted in Figure 3, for three different values of the surface magnetic fields, covering a time interval of 1000 yr. The plot shows that most of the nebulae fit in between model B (1 G) and model C (5 G.). Therefore, magnetically-driven winds can, in principle, solve the PPN problem (Bujarrabal et al. 2001), in which the linear momenta and kinetic energies associated with these nebulae are far too large to be powered by radiation pressure.

The other important point that comes out of this study is that magnetically-driven winds are able to shorten the transition time between the AGB and PN phases. For example, a late-AGB star with $1 M_{\odot}$ can evolve into a PN central star of $0.6 M_{\odot}$ in only 5000 yr for model C (5 G) and in 24,000 yr for model B (1 G). These numbers are smaller than previous studies which only take into account radiation pressure (Villaver, Manchado, & García-Segura 2002).

Therefore, we conclude that mass-loss rates of post-AGB stars and transition times from late AGB stars up to planetary nebula central stars could be directly linked to the production of magnetic field at the stellar core.

We thank Michael L. Norman and the Laboratory for Computational Astrophysics for the use of ZEUS-3D. The computations were performed at Instituto de Astronomía-UNAM. This work has been partially supported by grants from DGAPA-UNAM (IN130698, IN117799 & IN114199) and CONACyT (32214-E).

José Franco: Instituto de Astronomía, Universidad Nacional Autónoma de México, Apartado Postal 70-264, 04510 México, D.F., México (pepe@astroscu.unam.mx).

Guillermo García-Segura and José Alberto López: Instituto de Astronomía, Universidad Nacional Autónoma de México, Apartado Postal 877, 22800 Ensenada, B.C., México (ggs, jal@astrosen.unam.mx).

REFERENCES

- Alcolea, J., Bujarrabal, V., Sánchez-Contreras, C., Neri, R., & Zweigle, J. 2001, *A&A*, 373, 932
- Blackman, E. G., Frank, A., Markiel, J. A., Thomas, J. H., & Van Horn, H. M. 2001, *Nature*, 409, 485
- Bujarrabal, V., Alcolea, J., Sánchez-Contreras, C., & Sahai, R. 2002, *A&A*, 389, 271
- Bujarrabal, V., Castro-Carrizo, A., Alcolea, J., & Sánchez-Contreras, C. 2001, *A&A*, 377, 868
- Clarke, D. A. 1996, *ApJ*, 457, 291
- Desmurs, J.-F., Sánchez-Contreras, C., Bujarrabal, V., Colomer, F., & Alcolea, J. 2002, in *IAU Symp. 206, Cosmic Masers: from Protostars to Black Holes*, eds. V. Migenes & M. J. Reid (San Francisco: ASP), in press (astro-ph/0109543)
- García-Segura, G. 1997, *ApJ*, 489, L189
- García-Segura, G., Langer, N., Różyczka, M., & Franco, J. 1999, *ApJ*, 517, 767
- García-Segura, G., & López, J. A. 2000, *ApJ*, 544, 336
- García-Segura, G., López, J. A., & Franco, J. 2001, *ApJ*, 560, 928
- Greaves, J. S. 2002, *A&A*, 392, L1
- Habing, H. J. 1996, *A&A Rev.*, 7, 97
- Jura, M., Chen, C., & Plavchan, P. 2002, *ApJ*, 574, 963
- Kwok, S., Purton, C. R., & Fitzgerald, P. M. 1978, *ApJ*, 219, L125
- Miranda, L. F., Gómez, Y., Anglada, G., & Torrelles, J. M. 2001, *Nature*, 414, 284
- Pascoli, G. 1997, *ApJ*, 489, 946
- Perinotto, M. 1983, in *IAU Symp. 103, Planetary Nebulae*, ed. D. Flower (Dordrecht: Reidel), 323
- Różyczka, M., & Franco, J. 1996, *ApJ*, 469, L127
- Sahai, R. 2002, in *Emission Lines from Jet Flows*, eds. W. Henney, W. Steffen, & A. C. Raga, *RevMexAA(SC)*, 13, 133
- Sahai, R., et al. 2002, *ApJ*, 573, L123
- Sánchez-Contreras, C., Bujarrabal, V., & Alcolea, J. 1997, *A&A*, 327, 689
- Schwarz, H. E., Aspin, C., Corradi, R. L. M., & Reipurth, B. 1997, *A&A*, 319, 267
- Smith, E. J., Tsurutani, B. T., & Rosenberg, R. L. 1978, *J. Geophys. Res.*, 83, 717
- Stone, J. M., & Norman, M. L. 1992, *ApJS*, 80, 753
- Villaver, E., Manchado, A., & García-Segura, G. 2002, *ApJ*, 571, 880
- Wilcox, J., & Ness, N. 1965, *J. Geophys. Res.*, 70, 1233